Effect of the Type of SAN in SAN/CPE Blend: Morphology, Mechanical, and Rheological Properties

I. J. HWANG,[2] B. K. KIM[1]

[1] Department of Polymer Science and Engineering, Pusan National University, Pusan 609-735, Korea

[2] Department of Industrial Chemistry, Kyungnam Junior College, Pusan 617-701, Korea

Received 27 January 1997; accepted 6 June 1997

ABSTRACT: The effect of the molecular weight and acrylonitrile (AN) content of the styrene-acylonitrile copolymer (SAN) on the morphology, mechanical, and rheological properties of SAN/chlorinated polyethylene (CPE) blends was studied. The interaction between dispersed particle and matrix is expected to be optimal at the 25% AN content of SAN. Phase inversion from a dispersion to a continuous phase appears to occur above 50 wt % CPE. Mechanical properties increased with molecular weight at a constant AN content of SAN. Morphological, mechanical, and rheological properties were more sensitive to the AN content, rather than the molecular weight of SAN. © 1998 John Wiley & Sons, Inc. J Appl Polym Sci **67:** 27–36, 1998

Key words: SAN/CPE blend; morphology; rheology; composite model

INTRODUCTION

The behavior of polymer blends has been extensively investigated during the last several decades. Of particular interest have been the miscibility behavior of polymer-polymer blends and the deformation or toughness behavior of blends containing immiscible rubber particles in a thermoplastic polymer matrix.

Recently, many kinds of rubber-modified thermoplastic polymers have been developed and used in industrial fields. By blending a rubber component with rigid polymers, the impact strength of the polymer is improved, while the other properties, for example, modulus and processability, are generally deteriorated. Therefore, it is very important for the development of rubber-modified polymers to find how to improve the impact strength without deterioration of the other properties.

Acrylonitrile-butadiene-styrene terpolymer (ABS) is a typical rubber-modified polymer which has long been commercialized. Physical properties of ABS are influenced by not only the rubber content, rubber particle size, and rubber size distribution but also molecular weight and acrylonitrile (AN) content of the matrix styrene-acrylonitrile copolymer (SAN).[1,2]

As the rubber, polybutadiene or its related rubber composition is often used. These rubbers show a high degree of unsaturation in the main chain, and consequently, they are sensitive to oxidation under the influence of light and/or oxygen. In order to overcome this problem, it has been suggested that the rubber be replaced in the polymer composition by a highly saturated rubber, such as ethylene-propylene-diene terpolymer.

SAN can readily blend with a number of other polymers including poly(ε-caprolactone),[3,4] polycarbonate,[5–9] poly(vinylidenefluoride),[10] nylon,[11] polypropylene,[12] poly(phenylacrylate),[13] polyvinyl chloride (PVC),[14–17] leading to molecular compositions. The use of either a styrene-butadiene-styrene (SBS) block copolymer or an emulsion-made methyl methacrylate–grafted rubber (MBS) alone failed to give any significant increase in the

Correspondence to: B. K. Kim.

Journal of Applied Polymer Science, Vol. 67, 27–36 (1998)
 CCC 0021-8995/98/010027-10

Table I Properties of Base Resins

Materials	M_w	Other Characteristics	Source
SAN1	60,000	AN content, 35%	Hyosung BASF
SAN2	80,000	AN content, 35%	Hyosung BASF
SAN3	102,000	AN content, 24%	LUCKY
CPE		CI content, 36%	DOW

toughness of brittle SAN, even at concentrations up to 50%; however, a combination of the two rubber modifiers (SBS and MBS) produced a strong synergistic toughening.[18]

This work considers the melt blends of SAN with chlorinated polyethylene (CPE). Three types of SAN having different molecular weight and/or different AN content were used. The subsequent effects on morphology and melt, mechanical, and viscoelastic properties were examined.

EXPERIMENTAL

The polymers used in this study are described in Table I. Resins were used after drying in a vacuum at 70°C for 24 h. Blends were prepared with a corotating twin screw extruder (Berstoff) with temperature ranges of 170 ~ 180°C. For blending, 1.0 phr organotin stabilizer, 0.6 phr calcium stearate, 0.6 phr epoxidized soybean oil, and 0.5 phr oxidized polyethylene wax were also added to the resins.

Extrudates were quenched in water and pelletized, followed by injection molding (Batten field Unilog 400). Injection molding was done with temperature ranges similar to that for extrusion.

The morphology of the blends was observed from scanning electron microscopy (SEM). SEM photographs were taken from the fractured surface of the injection-molded tensile specimen (in liquid nitrogen) and the notched Izod impact specimen (at room temperature) and sputtered with gold before viewing.

Tensile properties were measured with a tensile tester (Tinius Olsen Series 1000), following the standard procedures described in ASTM D-638, at a crosshead speed of 5 mm/min. Impact strength was determined with a notched $\frac{1}{8}$-inch specimen (ASTM D-256). The above test was made at room temperature. At least five runs were made to report the average.

The melt properties of the blends were measured with a Rhometrics Dynamic Spectrometer (RDS, Type II) at 180°C with 10% strain, which is the upper limit of linear viscoelastic behavior. A temperature sweep was done from −100°C to 160°C with a stick bar sample at 2°C/min, 0.2% strain, and 6.28 rad/s.

RESULTS AND DISCUSSION

Morphology

Figures 1 and 2 show SEM micrographs of SAN/CPE blends. The blends show two-phase morphology at all compositions, that is, particle in matrix or cocontinuous structure. In addition, many holes, that is, traces of pull-out of dispersed phase after fracture, are observed. The poor interface should be due to the weak interfacial adhesion between SAN and CPE. However, for SAN3/CPE blends with 50 wt % CPE or more, it is difficult to identify dispersed phase from a continuous one. We may assume that CPE forms dispersed phase because of its higher viscosity relative to SAN.[19] Comparing symmetric composition for SAN1/CPE blends, that is, 70/30 versus 30/70, the domain sizes of the 30/70 blend are smaller than those of 70/30. This, among many factors, is the result of the greater melt viscosity of CPE as compared with SAN. With larger dispersed-phase viscosity, fine break-up would be more difficult.[20]

The rubber particles are dislodged from the matrix and show the formation of shear yielding during impact fracture [Fig. 2(a–d)]. At 60/40 and 50/50 compositions, SAN1/CPE blends and SAN3/CPE blends are clearly different in certain topological features of their impact fracture sur-

Figure 1 SEM micrographs of the fractured surface of the injection-molded tensile specimens for SAN/CPE blends: (a) SAN1/CPE (70/30), (b) SAN1/CPE(50/50), (c) SAN1/CPE(30/70), (d) SAN2/ CPE(70/30), (e) SAN2/CPE(50/50), (f) SAN3/CPE(70/30), (g) SAN3/CPE(50/50), and (h) SAN3/CPE(30/70).

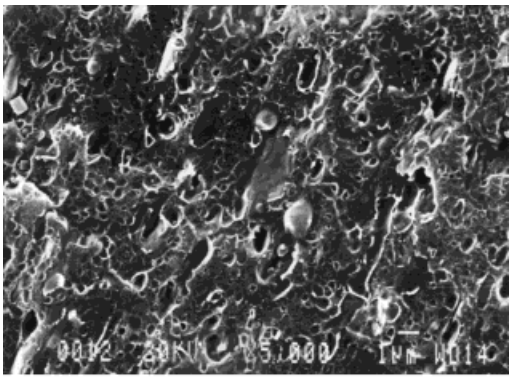

(a)

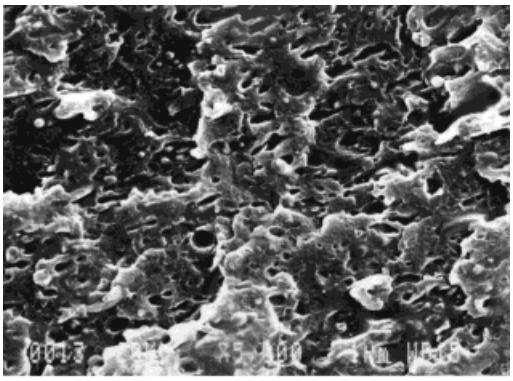

(b)

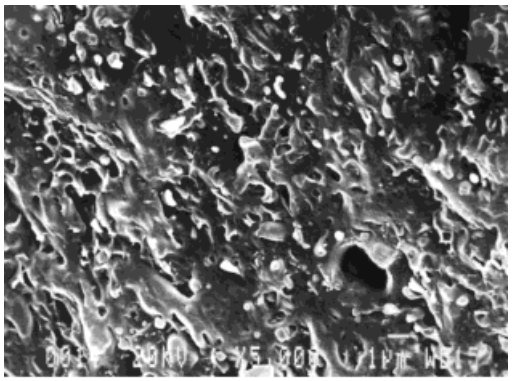

(c)

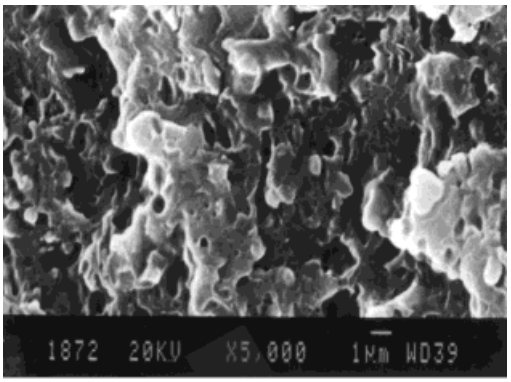
1872 20KV X5,000 1μm WD39

(d)

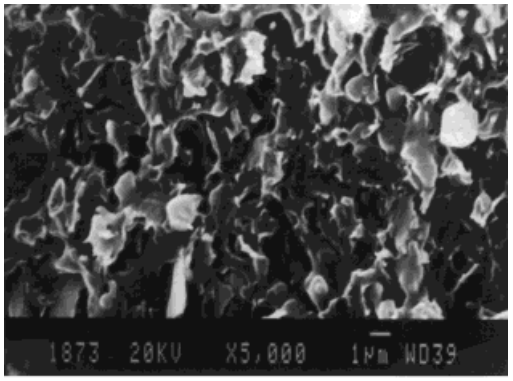
1873 20KV X5,000 1μm WD39

(e)

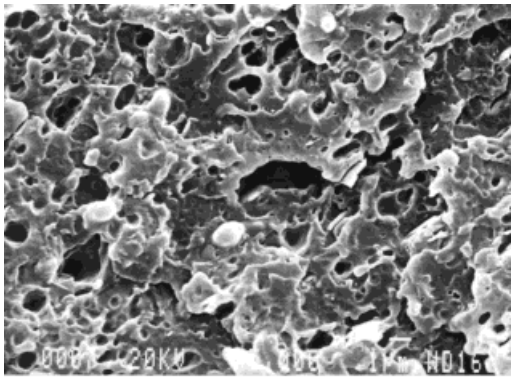

(f)

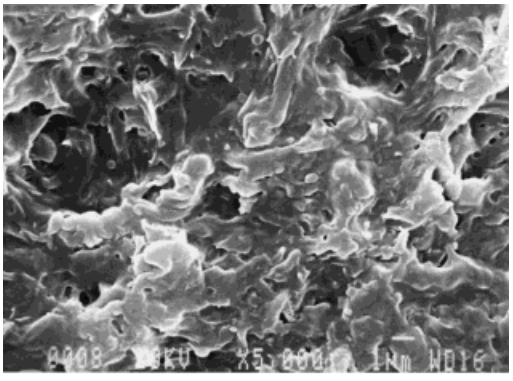

(g)

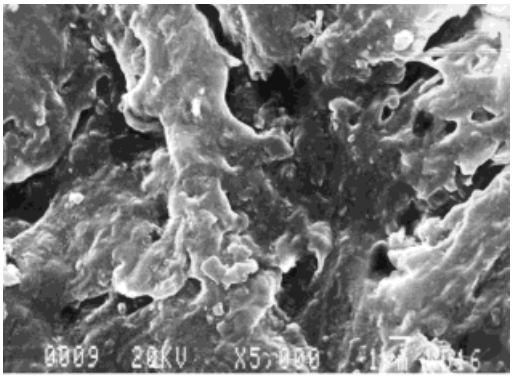
0009 20KV X5,000

(h)

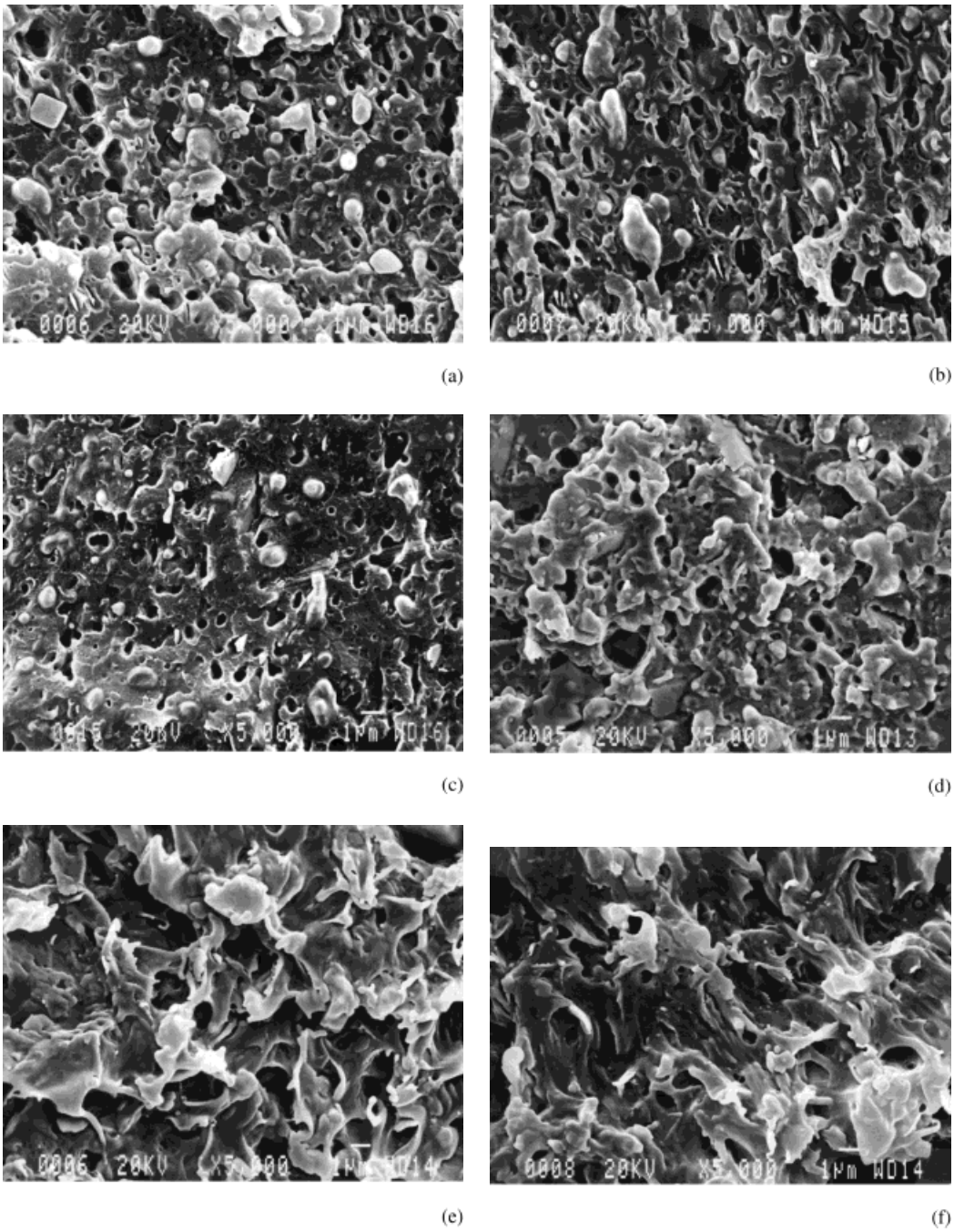

Figure 2 SEM micrographs of a notched impact fracture surface for SAN/CPE blends: (a) SAN1/CPE(70/30), (b) SAN1/CPE(60/40), (c) SAN1/CPE(50/50), (d) SAN3/CPE(70/30), (e) SAN3/CPE(60/40), and (f) SAN3/CPE(50/50).

face. It appears to be continuous in SAN3/CPE blends but clear in SAN1/CPE blends (Fig. 2). It seems that SAN3 can mix with CPE better than SAN1. This may be attributed to the finding that AN content in SAN3 is less than AN content in SAN1, resulting in lower cohesion in SAN3 and leading to the easier mixing of SAN3 and CPE. Kim et al. found that PVC is miscible with 11.5 $\sim$ 26 wt % AN-containing SAN.[15]

Mechanical Properties

Impact strength of the blends as a function of CPE content is shown in Figure 3. The impact strength

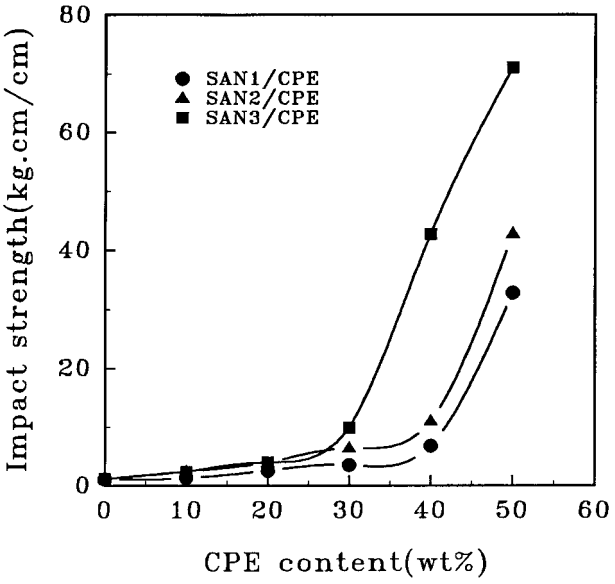

Figure 3 Notched Izod impact strength versus composition.

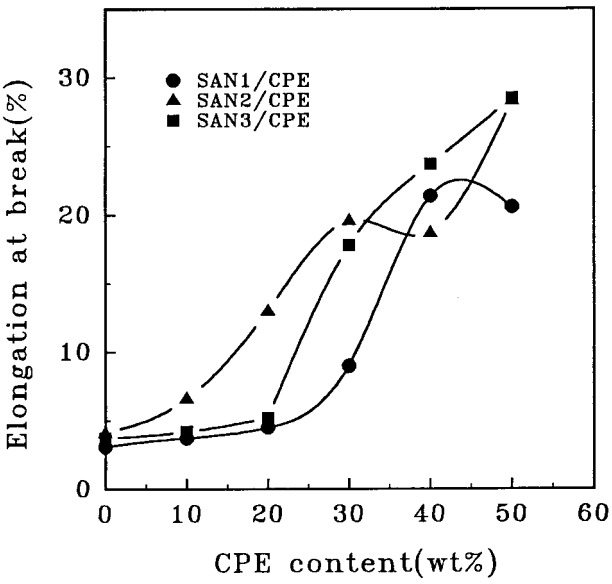

Figure 5 Elongation at break versus composition.

of the blends increases with CPE content, with the effect more pronounced as the molecular weight of SAN increases. A brittle-tough transition in the impact strength is observed at a composition of about 40 wt % CPE (SAN1 and SAN2) and about 30 wt % CPE (SAN3). Below 30 or 40 wt % CPE, a gradual increase in impact strength is observed with increasing CPE content, but the effect is small compared with the transition.

Figures 4 and 5 show the tensile strength and the elongation at break of the blends as a function of CPE content. The tensile strength decreases almost linearly with CPE content, indicative of good dispersion of CPE in SAN without the inclusion of SAN in CPE domains. The elongation at break is increased with CPE content. SAN2 and SAN3 blends give slightly more improvement in this property than SAN1. The better mechanical properties of these blends are attributed to the superior mechanical properties of SAN2 and the better compatibility of SAN3 with CPE.

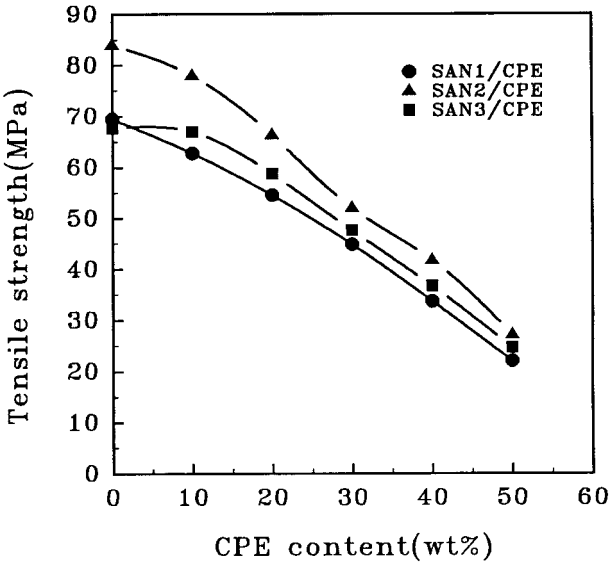

Figure 4 Tensile strength versus composition.

Modulus Behavior at 25°C

A decrease of modulus with an increase of the CPE content was observed for the three types of SAN/CPE blends studied (Fig. 6). The three types of SAN/CPE blends did not cause any significant difference in the concentration dependence of the elastic modulus.

The model of Kerner was used to describe the concentration dependence of elastic modulus[21]:

$$E^{\text{rel}} = (1 + AB\varphi_{\text{CPE}})/(1 - B\varphi_{\text{CPE}}) \quad (1)$$

$$A = (7 - 5\nu_m)/(8 - 10\nu_m) \quad (2)$$

$$B = (E_e/E_m - 1)(E_e/E_m + A) \quad (3)$$

Poisson's ratios for SAN and CPE are taken as 0.33 and 0.499, respectively. The parameters A and B of the Kerner equation were calculated with CPE as inclusions in one case and matrix in the other because a phase inversion from a dispersed to a continuous phase appears to occur above 50

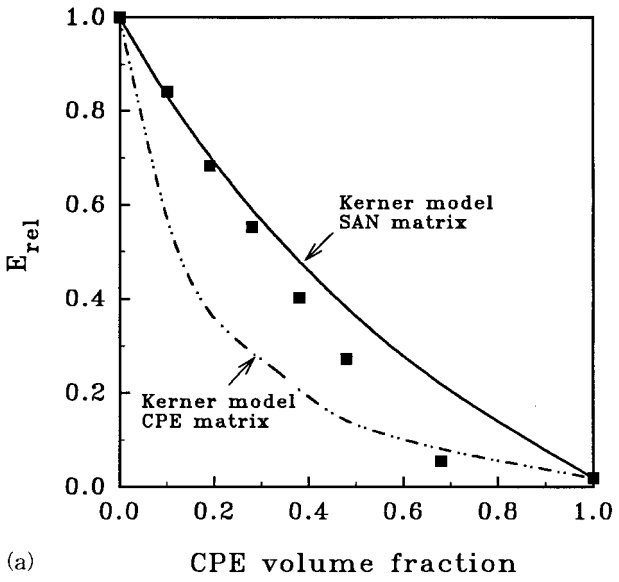

(a)

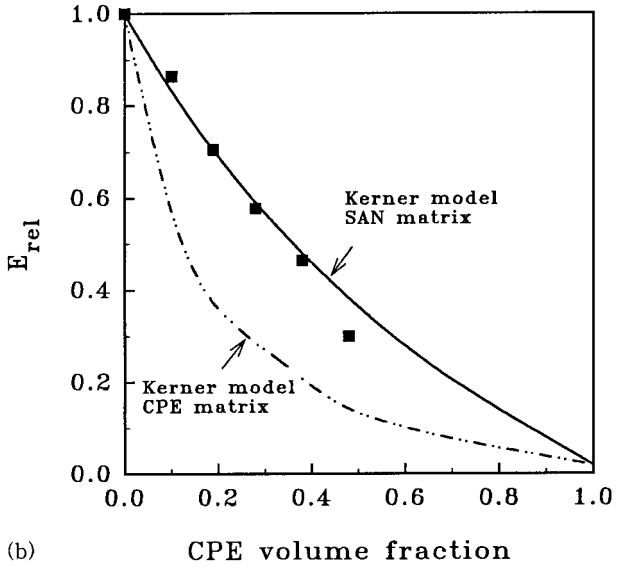

(b)

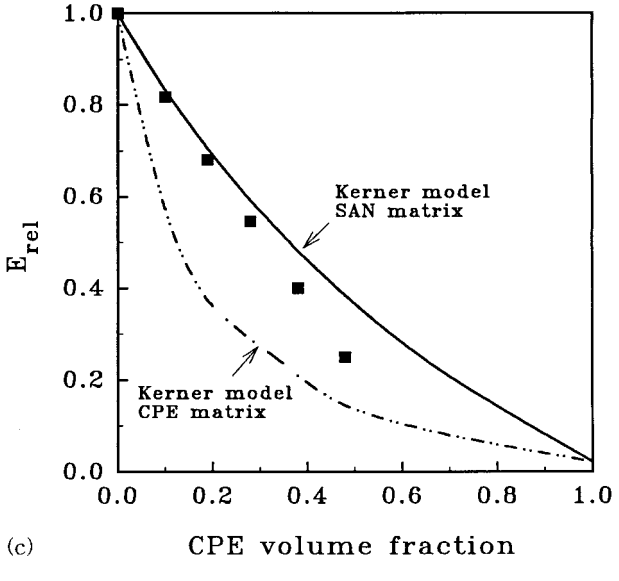

(c)

vol %. One can see that this model gives a fairly good agreement.

A number of theoretical composite models for predicting the modulus behavior are available. These models help in evaluating such features as phase interaction, phase continuity, and phase inversion. The parallel-series models[22] are often used for establishing the upper and lower bounds on the composite modulus.

$$G_{\text{blend}} = \varphi_1 G_1 + \varphi_2 G_2 \quad \text{parallel model} \tag{4}$$

$$G_{\text{blend}} = (\varphi_1/G_1 + \varphi_2/G_2)^{-1} \quad \text{series model} \tag{5}$$

A dual-phase continuity model,[23] which also considers phase interactions, is derived by Davies:

$$(G_{\text{blend}})^{1/5} = \varphi_1 G_1^{1/5} + \varphi_2 G_2^{1/5} \tag{6}$$

Finally, the one-parameter Coran-Patel model,[24] which represents a phenomenological interplay between the series and the parallel models, can be expressed as

$$G_{\text{blend}} = \varphi_2^n (n\varphi_1 + 1)(G_H - G_L) + G_L \tag{7}$$

where

$$G_H = \varphi_1 G_1 + \varphi_2 G_2 \quad \text{and}$$

$$G_L = [(\varphi_1/G_1) + (\varphi_2/G_2)]^{-1} \tag{8}$$

In the above equations, G_{blend}, G_1, and G_2 represent the modulus of the blend and constituents 1 and 2, respectively.[25] φ_1 and φ_2 represent the volume fraction of constituents 1 and 2, respectively.

As shown in Figure 7, the models generally fail to predict the modulus behavior over the entire range of composition. The Coran-Patel model fits the data best in the range of $n = 1.5 \sim 2.0$. The fitting parameter (n) can be related to phase inversion and other physical parameters. For systems of variable morphology, $(n - 1)/n$ probably indicates the approximate center of range of volume fractions φ_2, where a phase transition or inversion takes place. Extending the above analysis to the material presented here, $(n - 1)/n$ gives $0.3 \sim 0.5$. The phase connectivity of CPE begins to form, $\varphi_{\text{CPE}} = 0.5 \sim 0.7$, which agrees well with our SEM morphology.

Figure 6 Elastic modulus versus volume fraction: (a) SAN1/CPE, (b) SAN2/CPE, and (c) SAN3/CPE.

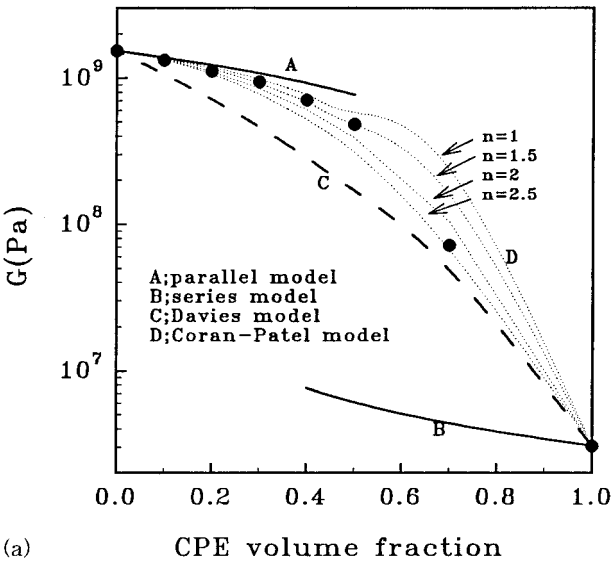

(a)

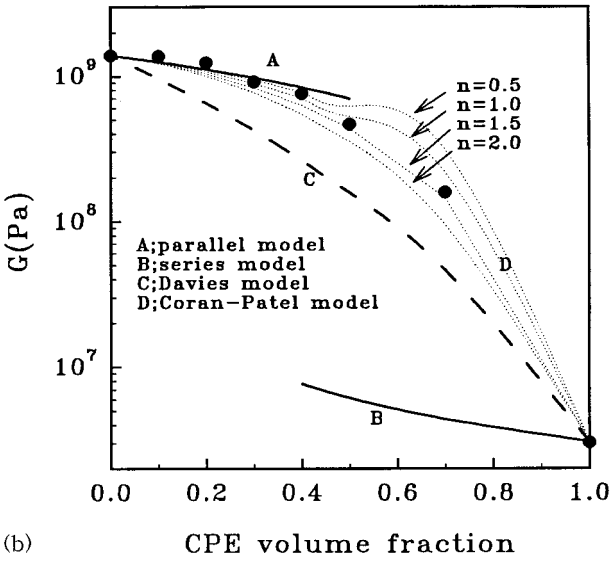

(b)

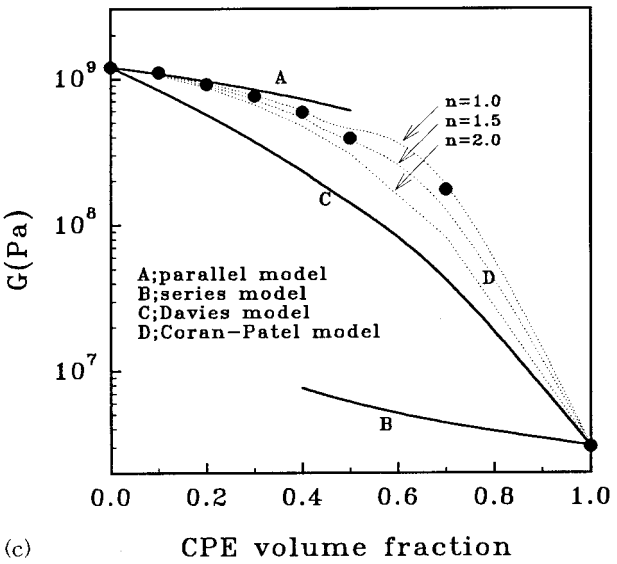

(c)

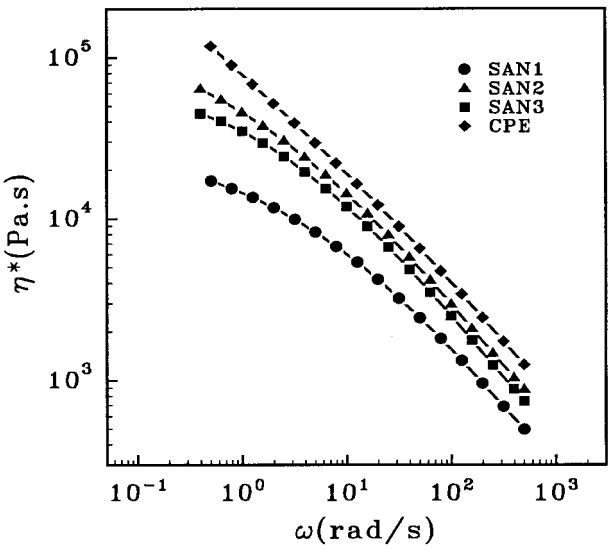

Figure 8 Melt viscosity versus frequency.

Rheological Properties

Viscosity is a very useful rheological function that describes a material in the molten state. Figure 8 shows the complex viscosity as a function of frequency for the pure materials. Viscosities of SAN2 and SAN3 are close to those of CPE throughout the frequency range tested. However, the viscosities of SAN1 are lower than those of CPE throughout. The difference in viscosity functions between the SAN1 and SAN2, especially at low frequency, is the response of the different molecular parameters, namely, molecular weight and molecular weight distribution.

Figure 9 shows the viscosity of the blend as a function of CPE content. The $\eta^*(\omega)$ value of SAN/CPE blends shows deviations from the log-additivity rule. The viscosities of SAN1/CPE blends generally follow the log-additivity rule; SAN2/CPE blends show negative deviation, and SAN3/CPE blends show positive deviation. In blends, negative deviation of viscosity is often obtained with an interfacial slip due to the poor interface interactions. However, positive deviation in viscosity is often obtained when there are strong interactions between dispersed domains or when the morphology has an interlocked structure.[19] This was clearly seen in the SEM micrographs.

Figures 10 and 11 show the storage modulus (G') and tan δ of the SAN2/CPE blends with varying rubber content. The data for SAN1/CPE

Figure 7 Modulus versus volume fraction: (a) SAN1/CPE, (b) SAN2/CPE, and (c) SAN3/CPE.

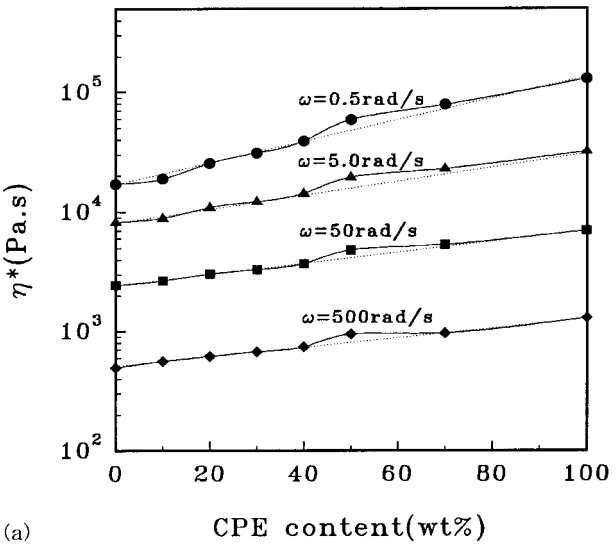

(a)

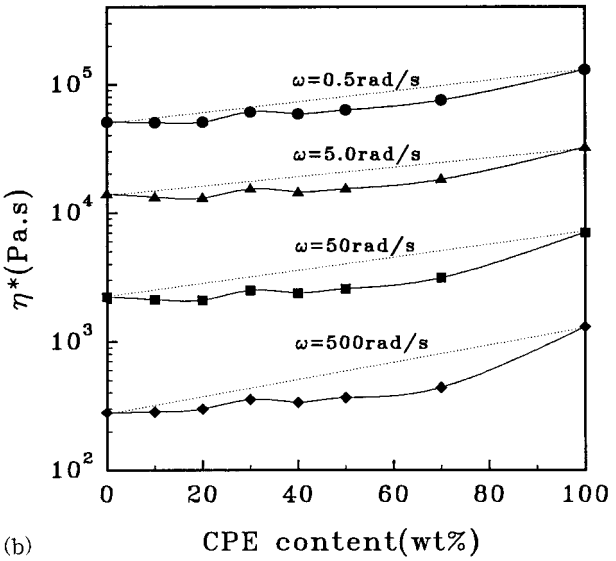

(b)

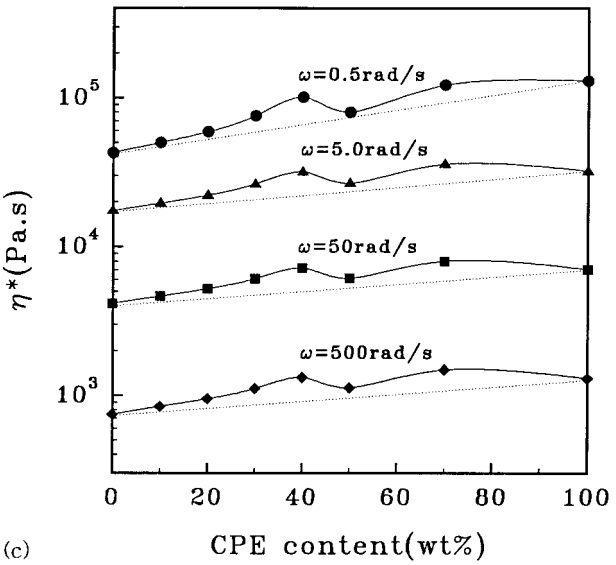

(c)

Figure 9 Viscosity versus composition: (a) SAN1/CPE, (b) SAN2/CPE, and (c) SAN3/CPE.

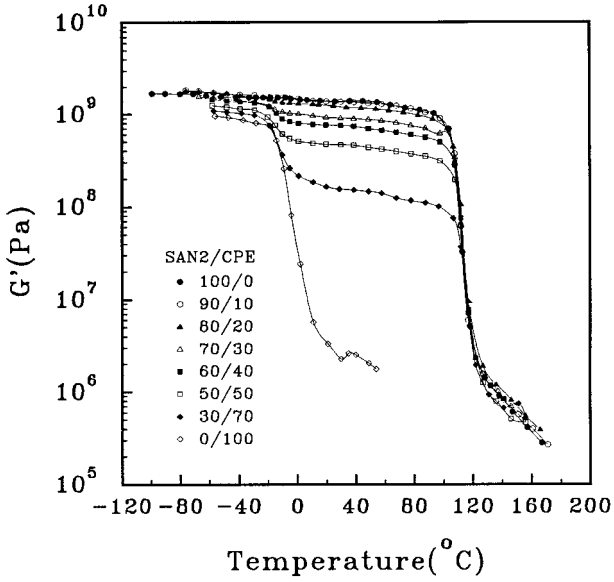

Figure 10 Storage modulus versus temperature.

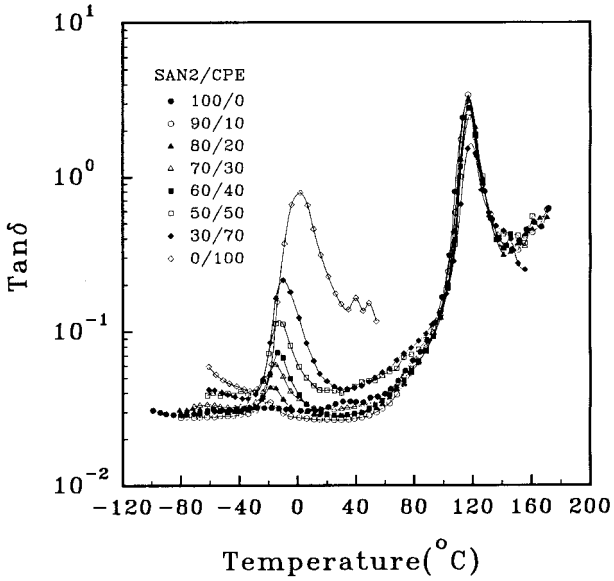

Figure 11 Loss tangent versus temperature.

and SAN3/CPE blends are not shown for clarity because they are essentially identical with those of SAN2/CPE blend. However, major relaxation temperatures recorded in three SAN/CPE blends are summarized in Figure 12 as a function of blend composition.

It is seen that SAN and CPE show relaxation at 116°C (tan δ) and 2°C, respectively. The lower

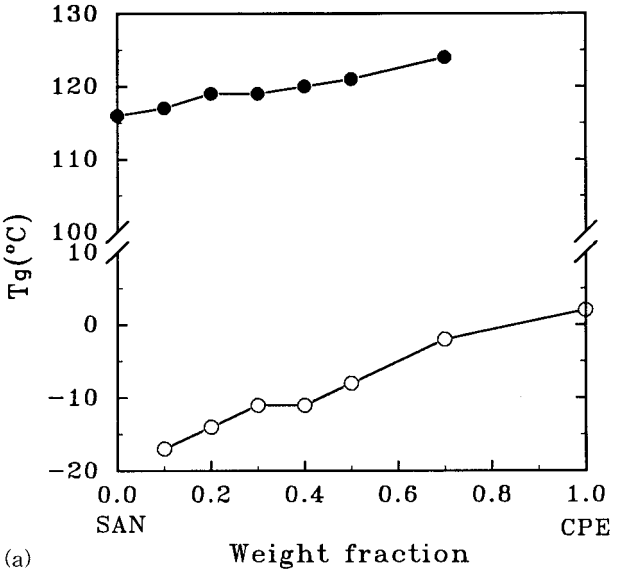

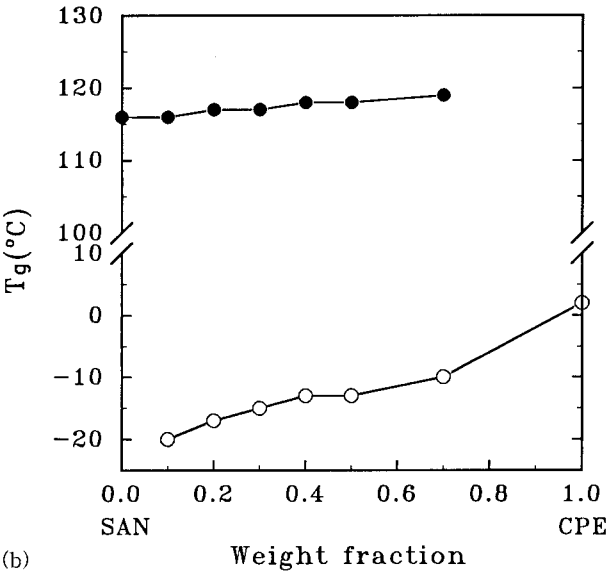

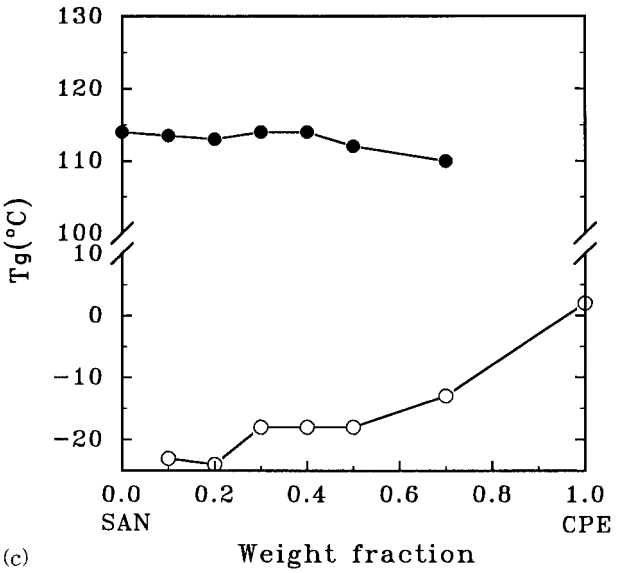

Figure 12 Relaxation temperatures in RDS measurement of SAN/CPE blends: (a) SAN1/CPE, (b) SAN2/CPE, and (c) SAN3/CPE.

T_g (CPE) moves toward the lower temperature by several degrees as the rubber content decreases, whereas the higher T_g (SAN) of the blend is higher than that of virgin SAN. Eventually, the T_g values of the blends move away from each other. It is conceivable that the partitioning of low-molecular-weight species, such as oligomers and various additives, during melt blending may contribute to the relative shifts in T_g for the blends.[26] The shift was also attributed to plasticization of the CPE phase by processing aids used in the preparation of the blends.[27]

REFERENCES

1. H. S. Kim, H. Keskkula, and D. R. Paul, *Polymer,* **32,** 1447 (1991).
2. M. E. Fowler, H. Keskkula, and D. R. Paul, *J. Appl. Polym. Sci.,* **37,** 225 (1989).
3. S. C. Chiu and T. G. Smith, *J. Appl. Polym. Sci.,* **29,** 1781 (1984).
4. S. C. Chiu and T. G. Smith, *J. Appl. Polym. Sci.,* **29,** 1797 (1984).
5. M. J. Guest and J. H. Daly, *Eur. Polym. J.,* **25,** 985 (1989).
6. D. Quintens and G. Groeninckx, *Polym. Eng. Sci.,* **31,** 1207 (1991).
7. D. Haderski, K. Sung, J. Im, A. Hiltner, and E. Baer, *J. Appl. Polym. Sci.,* **52,** 121 (1994).
8. J. D. Keitz, J. W. Barlow, and D. P. Paul, *J. Appl. Polym. Sci.,* **29,** 3131 (1984).
9. R. A. Mendekson, *J. Appl. Polym. Sci.,* **23,** 1975 (1985).
10. J. M. Machado and C. S. Lec, *Polym. Eng. Sci.,* **34,** 59 (1994).
11. B. Majumdar, H. Keskkula, and D. R. Paul, *Polymer,* **35,** 4263 (1994).
12. S. N. Maiti, V. Agarwal, and A. K. Guipia, *J. Appl. Polym. Sci.,* **43,** 1891 (1991).
13. D. Rana, B. M. Mandal, and S. N. Bhatlacharyya, *Polymer,* **34,** 1454 (1993).
14. J. C. Huarng, K. Min, and J. L. White, *Polym. Eng. Sci.,* **28,** 1590 (1988).
15. J. H. Kim, J. W. Barlow, and D. R. Paul, *J. Polym. Sci.,* **B27,** 2211 (1989).
16. P. P. Lizymol and S. Thomas, *J. Appl. Polym. Sci.,* **51,** 635 (1994).
17. J. C. Muarng, K. Min, and J. L. White, *Polym. Eng. Sci.,* **28,** 1085 (1988).

18. M. E. Fowler, H. Keskkula, and D. R. Paul, *J. Appl. Polym. Sci.,* **35,** 1563 (1988).
19. C. D. Han, *Multiphase Flow in Polymer Processing,* Academic, New York, 1981.
20. B. D. Favis and J. P. Chalifoux, *Polymer,* **29,** 1761 (1988).
21. J. Jancar, A. DiAnselmo, A. T. DiBenedetto, and J. Kucera, *Polymer,* **34,** 1684 (1993).
22. M. Takayanagi, H. Harima, and Y. Iwata, *Mem. Fac. Eng. Kyushy Univ.,* **23,** 1 (1963).
23. W. E. A. Davies, *J. Phys. (D),* **4,** 318 (1971).
24. A. Y. Coran and R. Patel, *J. Appl. Polym. Sci.,* **20,** 3005 (1976).
25. J. K. Yeo, L. H. Spering, and D. A. Thomas, *Polym. Eng. Sci.,* **21,** 696 (1981).
26. M. J. Guest and J. H. Daly, *Eur. Polym. J.,* **25,** 985 (1989).
27. A. Tse, R. Laakso, E. Baer, and A. Hiltner, *J. Appl. Polym. Sci.,* **42,** 1205 (1991).